Are RFID Sensing Systems Ready for the Real World?

Ju Wang
University of Waterloo
Waterloo, Ontario, Canada
ju.wang@uwaterloo.ca

Liqiong Chang
University of Waterloo & Northwest University
Waterloo, Ontario, Canada
liqiong.chang@uwaterloo.ca

Omid Abari
University of Waterloo
Waterloo, Ontario, Canada
omid.abari@uwaterloo.ca

Srinivasan Keshav
University of Waterloo
Waterloo, Ontario, Canada
keshav@uwaterloo.ca

ABSTRACT

Passive Radio Frequency IDentification (RFID) tags are commonly used to provide Radio Frequency (RF) accessible unique identifiers for physical objects due to their low-cost, lack of battery, and small size. Besides this basic function, many novel RFID-based sensing applications have been proposed in the last decade, including localization, gesture sensing, and touch sensing, among others. Nevertheless, none of these systems are in widespread use today. We hypothesize that this is because the accuracy of these systems does not meet application requirements when there are even minor changes in the RF environment or in tag geometry, i.e., changes in a tag's orientation or flexing.

This paper uses both theoretical analysis and real-world experiments to test this hypothesis. Our theoretical analysis shows that even a small phase or RSS noise level can result in significant estimation errors. Our extensive real-world experiments find that both the absolute and differential values of phase and RSS readings of an RFID tag's signal can vary as much as by π radians and 10 dB, respectively, due to small changes in the tag's orientation or flexing. Because of these large variations, RFID-based application systems relying on the signal phase or RSS cannot meet application requirements, confirming our hypothesis. In addition to this strong negative result, we also present some insights into designing robust RFID systems that are suitable for use in the real world.

CCS CONCEPTS

• Human-centered computing → Ubiquitous and mobile computing systems and tools; **Empirical studies in ubiquitous and mobile computing**; **• Applied computing →** *Engineering*.

KEYWORDS

RFID; Robustness; RSS; Phase.

MobiSys '19, June 17–21, 2019, Seoul, Republic of Korea

ACM ISBN 978-1-4503-6661-8/19/06…$15.00
https://doi.org/10.1145/3307334.3326084

ACM Reference Format:
Ju Wang, Liqiong Chang, Omid Abari, and Srinivasan Keshav. 2019. Are RFID Sensing Systems Ready for the Real World?. In *The 17th Annual International Conference on Mobile Systems, Applications, and Services (MobiSys '19), June 17–21, 2019, Seoul, Republic of Korea.* ACM, New York, NY, USA, 12 pages. https://doi.org/10.1145/3307334.3326084

1 INTRODUCTION

RFID technology allows a *reader* to query a unique identification code embedded in either an active or a passive[1] *tag* over an RF channel. It is widely used for smart identification, where a tag is attached to a physical object, such as baggage, clothing, or a transit token, and the reader identifies the object based on its ID [18]. Due to their low-cost (a few cents each), lack of battery, and small size, passive RFID tags are in widespread use; their market value is expected to rise to $14.9 billion by 2022 [27].

Beyond the traditional identification and authentication functions of RFID systems, many RFID-based applications and systems have been proposed in recent research, including decimeter-level localization and tracking [45], fine-grained gesture/activity recognition [9, 10], touch sensing [26], orientation sensing [43], and device-free sensing [47], amongst many others [7, 8, 46]. These systems typically rely on detecting modifications to a tag's response, such as a change in Received Signal Strength (RSS) or phase. For example, in a touch-sensing application, the reader detects that a tag has been touched due to a change in its RSS and phase values [26].

Despite extensive work in this area for the last ten years or so, novel uses of RFID tags have rarely progressed beyond research prototypes, with nearly no usage in practice. We hypothesize that *RFID-based sensing systems are not widely used in practice because they are not robust to even minor variations in the environment or tag geometry.* This hypothesis is motivated by our observation that it is possible to achieve decimeter-level localization accuracy *only* when the RF environment is stable (i.e., no people are moving) and the tag is always facing the reader's antenna head-on and is not rotated. Similarly, when used for gesture sensing [9, 10], we can reliably identify gestures *only* when the environment is stable and the human target stands at a fixed location and repeats the exact same gesture.

The goal of this paper is to validate our research hypothesis. We also want to determine how to make novel RFID systems robust enough to be used in practice. To do so, we first survey several

[1] Active tags need a source of energy; passive tags have no battery and harvest energy from a reader's RF signal.

RFID-based applications and mathematically model the relationship between phase and RSS readings and an application's accuracy. We find that even a small phase noise level of 0.5 radians or a small RSS noise level of 2 dB can result in up to a 32° angle estimation error or a 1.1 m range estimation error. This is corroborated by extensive real-world experiments for seven different use cases and four different environments, demonstrating that even when the distance between a tag and a reader is fixed, both the absolute and differential values of phase and RSS readings of an RFID tag can vary by as much as π radians and 10 dB, respectively, due to changes in the tag's orientation and geometry. Based on these observations, we conclude that RFID-based application systems are bound to suffer large errors in practice due to these variations, validating our hypothesis.

Although we find that most existing RFID-based applications are not robust in practice, this does not mean that all RFID-based applications are destined to be fragile. Instead, based on our experimental results, we show how to improve the robustness of RFID systems by using stable signal features and carefully selecting a right type of tags for each application.

We make the following contributions:

- We comprehensively survey research into passive RFID-based applications and find that the phase and RSS are the most widely used signal parameters.
- We use theoretical models to study the impact of phase and RSS noise on the accuracy of the angle and range estimations of RFID systems.
- We conduct an extensive experimental campaign and find that large phase and RSS variations are unavoidable in practice.
- We present insights into designing robust RFID systems.

Paper outline: We present background regarding RFID systems, RSS and phase measurements in Section 2. A survey of existing RFID applications and an evaluation of their resilience to phase and RSS noise is in Section 3. We discuss experiments to determine how much phase and RSS readings vary in realistic settings in Section 4. We discuss how to improve the robustness of RFID systems in Section 5. This work is concluded in Section 6.

Raw experimental data: We have made our testing software and all raw experimental data openly available at https://www.dropbox.com/s/z34h0lk7bc8x0p0/Raw-data-and-Software-code.zip?dl=0

2 BACKGROUND

Fig. 1 shows a typical passive RFID system, which consists of two parts: a reader and a tag. The reader transmits an RF signal as a query. The tag uses this query to power up and respond with its ID. Since passive tags have no battery, RFID readers use a directional antenna to focus their power and increase their reading range. Besides the ID, commodity RFID readers also measure two RF parameters related to the tag's signal: Received Signal Strength (RSS) and Received Signal Phase (RSP), discussed next.

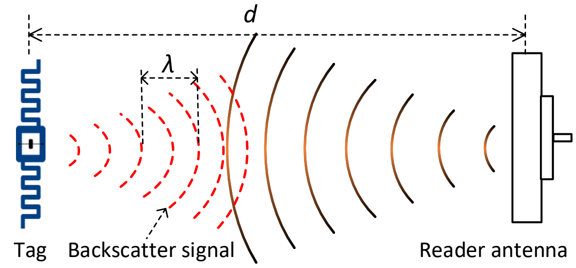

Figure 1: Illustration of a passive RFID system.

2.1 Received signal strength

RSS is the power of the tag's signal received by an RFID reader. Since RFID communicates using backscatter radio, which is fundamentally different from conventional radio (e.g., Wi-Fi radio), we model the RSS reading R in dB using the monostatic backscatter link budget introduced by Griffin *et al.* [14], as follow:

$$R(dB) = 10\log\left[\frac{C_G \cdot C_M \cdot C_P \cdot \lambda^4}{(4\pi d)^4 \cdot \xi^2} P_{tx}\right], \tag{1}$$

where, d is the distance between the tag and the reader's antenna; λ is the wavelength of the RFID signal; P_{tx} is the reader's transmission power; C_G, which is a constant, is related to the antenna gains of the reader and the tag; C_M is the modulation factor, which is a constant for a given reader; C_P is related to the polarization mismatch between the tag and the reader; and ξ is the path loss factor that related to the environment. For a given environment and deployment setup, C_P and ξ also are constant. Thus, Eqn. (1) can be simplified to:

$$R(dB) = 10\log\left[\frac{C \cdot P_{tx} \cdot \lambda^4}{d^4}\right], \tag{2}$$

where, $C = C_G C_M C_P / (4^4 \pi^4 \xi^2)$ is a constant.

Eqn. (2) shows that the RSS is a function of the distance between a tag and a reader's antenna. It is worth noting that this expression models not only line-of-sight, free-space scenarios but also non-line-of-sight, real-world scenarios with appropriate selection of parameters such as the polarization mismatch value C_P and the path-loss factor ξ.

2.2 Received signal phase

RSP is the phase of the tag's signal when received by a reader. In *free-space*, the RSP is given by [20]:

$$\phi = \left(\frac{2\pi}{\lambda} 2d + C'\right) \bmod 2\pi, \tag{3}$$

where, d is the distance between the tag and the reader's antenna, λ is the signal's wavelength, C' is a constant which represents the additional phase offset introduced by hardware of tags and reader antennas. The expression shows that the phase is a function of the distance between the tag and the reader's antenna. However, in reality, the phase can also be affected by multipath effects, channel conditions, and among other factors.

In summary, the values of the RSS and RSP parameters measured by a tag reader depend on the distance between the tag and the reader. Thus, by measuring these parameters, it is possible to estimate the distance between a reader and a tag. This has been exploited for applications, such as localization and gesture identification. In the next section, we discuss these applications in more details.

3 RFID APPLICATIONS

In this section, we first present a survey of RFID-based applications and systems. We also explain how these systems utilize phase and RSS measurements. Then, we evaluate their resilience to phase and RSS noise using standard theoretical models.

3.1 A Survey of RFID Applications

In the past few years, many RFID systems have been designed in the research community, targeting a wide range of applications. We survey these next.

3.1.1 Localization & Tracking. A common use of RFID tags is to track and localize objects. For example, libraries can attach tags to books in order to locate misplaced books and also to automate the checkout process. Hospitals can use RFID tags to localize and track their equipment. Tagging can also help them to manage their inventory.

Most RFID-based localization systems use either mathematical models or training schemes to track or localize a tag. For example, Zhou *et al.* [48] first use the training scheme to map RSS measurements to the locations of a tag. Then, they use the trained data set to estimate the location of a tag from its RSS measurements. In contrast, the system proposed by Sanpechuda *et al.* [29] takes a different approach, deploying reference tags in many known locations. Then, it compares the RSS of a moving tag with the RSS of reference tags to estimate its location with respect to references. However, both systems have limited accuracy as they only rely on the coarse-grained RSS measurement.

In order to achieve a higher localization accuracy (e.g., decimeter-level), recent systems measure the tag's phase information at multiple antennas or multiple frequencies, and then use the phased-antenna array model to estimate the Angle-of-Arrival (AoA) [17] or the Time-of-Flight (ToF) [41] of a tag's signal. Although this technique improves the localization accuracy, it works poorly in multi-path environments. Since the estimated AoA or ToF might be different from the true direction or the true distance (i.e., time-of-flight) of the tag with respect to the reader. To combat the multi-path problem, other recent studies use both the phase and RSS information [39, 40], and mathematical models to localize tags. For example, PinIt [40] uses the Synthetic Aperture Radar (SAR) model and compares the multi-path profile of a tag with reference tags to localize the tag with higher accuracy.

3.1.2 Ordering. Another use-case of RFID tags is to find the relative ordering of multiple objects. These applications determine only the relative locations of tags rather than their absolute locations. For example, to find a misplaced book on a library shelf, one needs to find the relative location of the book with respect to other books. OTrack [32] finds relative locations of tags using RSS readings. The work proposed in Reference [33] uses the spatial-temporal profiling of phase values to order tags in a two-dimensional space. However, this system fails in multipath environments. To combat the multipath effect, MobiTagbot [30] first detects multipath effects by using the phase information of multiple channels, and then it excludes phase readings that are distorted by the multipath effect.

3.1.3 Gesture & Activity Recognition. Some recent papers use RFID tags for gesture and activity recognition [9, 10]. By attaching tags to the human body and monitoring phase and RSS changes, they can identify body gestures or activities. For example, FEMO [13] monitors exercise activities by attaching RFID tags to dumbbells. Similarly, ShopMiner [35] monitors customer shopping behavior by using the phase measurements of tags attached to clothing. Pantomime [34] relies on phase measurements from multiple tag-arrays for a gesture-based interaction application.

3.1.4 Touch Sensing. Another application of RFID tags is to use them for battery-free touch sensing [26, 28]. Specifically, when a user touches the tag's antenna, the impedance of the antenna changes. This results in a change in the tag's phase and RSS readings which can be sensed by the RFID reader. For example, IDSense [24] attaches tags to objects and identifies two touch events (swipe touch and cover touch) by detecting the changes in the tag's phase and RSS information. PaperID [23] detects more than five types of touch events by applying a supervised machine learning method to the phase and RSS data. However, these systems can only detect coarse-grained gestures. A recent system, i.e., RIO [26], detects the fine-grained finger touch gestures by comparing the phase changes caused by the finger against pre-calibrated phase data.

3.1.5 Orientation Sensing. Phase and RSS measurements of an RFID tag change depending on the tag's orientation. Therefore, another application of RFID systems is to use RFID tags as orientation sensors [31, 43]. For example, Gupta *et al.* [15] estimate the 1D orientation of a tag by tracking the tag's RSS fluctuations. Shirehjini *et al.* [36] determine the 2D orientation of a target (e.g. robot and chair) by using a site-survey approach for both the RSS and phase measurements. Tagyro [43] attaches an array of multiple tags to a target and estimates the target's 3D orientation by using the phase offsets between tags.

3.1.6 Device-free Sensing. Unlike the applications discussed above, device-free sensing systems do not require the object to carry any tag. These systems use the phase and RSS changes induced by an object on multiple tags that are attached to the environment to localize and sense an object. For example, Tadar [47] detects the movement of a target by using both phase and RSS readings of multiple tags attached to a wall. D-Watch [42] uses a similar approach to localize a human target, using multiple tags that are randomly deployed in a room. GRfid [49] uses the phase information of tags for device-free gesture sensing. R# [12] estimates the number of people in a space by measuring the RSS variances of tags. TagScan [41] identifies the material type of an object using the phase and RSS measurements of tags that are deployed near it.

3.1.7 Other Sensing Applications. Beyond the applications discussed above, there are many other RFID-based sensing applications. For example, to estimate the vibration frequency of an engine, Tagbeat [46] attaches an RFID tag to the engine and measures its phase change. Reference [8] detects the liquid volume in a glass by attaching multiple tags to the glass and comparing their RSS values. Sarma *et al.* [7] use RFID tags to detect the failure of a freezer. Specifically, they can detect if ice is melting by attaching a tag to it and monitoring the change in the RSS readings.

3.2 Resilience to RSS and Phase Variations

All of the RFID-based applications in our comprehensive survey rely on measurements of the phase and/or RSS readings of tags to infer the distance and angle between a tag and a reader. This distance or angle information is then directly or indirectly used for localization, gesture sensing, vibration sensing, and so on. Therefore, the quality of the phase and RSS information is critical for the accuracy of RFID-based applications.

We next discuss the impact of phase/RSS noise on the accuracy of RFID-based range and angle estimations. Specifically, we first introduce an RSS-based range estimation model and a phase-based angle estimation model. Then, we analyze the range and angle errors introduced by phase/RSS noise by using, first, theoretical models, and subsequently, numerical results.

3.2.1 RSS-based Range Estimation. The range model estimates the distance between a tag and a reader using the tag's RSS measurements. Specifically, for a given environment and deployment setup, the tag-to-reader distance d can be estimated, based on Eqn. (2), as follow:

$$d = 10^{-\frac{R}{40}} \cdot \lambda \cdot \sqrt[4]{C \cdot P_{tx}}, \tag{4}$$

where, R is the tag's RSS measurement, λ is the wavelength of the RFID signal, P_{tx} is the reader's transmission power, and C is a constant and defined in Eqn. (2). By using this model, we can define the distance error ratio as follow:

$$E_d = |1 - \frac{d_2}{d_1}| = |1 - 10^{-\frac{\Delta R}{40}}|, \tag{5}$$

where, d_1 and d_2 are estimated distances using the true RSS measurement (R_1) and the noisy RSS measurement (R_2), respectively, and $\Delta R = |R_2 - R_1|$ is RSS noise. Eqn. (5) implies that E_d is independent of the reader's transmission power, the channel frequency (i.e., wavelength) and the antenna properties.

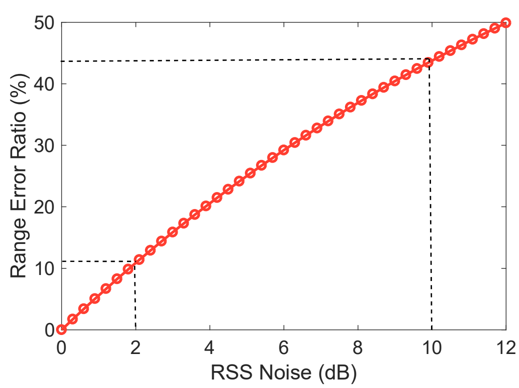

Figure 2: Impact of RSS noise on the range error ratio.

Fig. 2 shows the relationship between the range error ratio and RSS noise. As can be seen, a 2 dB and a 10 dB RSS noise level would result in ∼11% and ∼44% distance errors, respectively. Note that a common reading range of an RFID tag is around 10 m. That is to say, the distance error for the 2 dB or 10 dB RSS noise level would be ∼1.1 m or ∼4.4 m, respectively, which exceeds the decimeter-level accuracy requirement of most localization/tracking applications, such as baggage sorting [45] or locating a misplaced book in a stack [40].

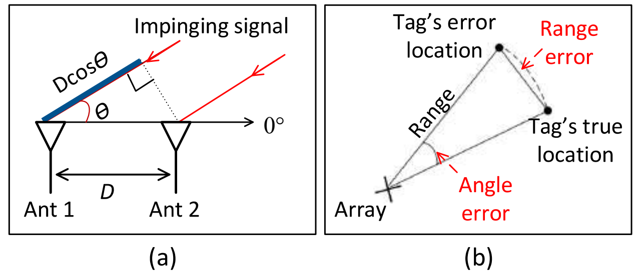

Figure 3: Illustrations of the phase-based angle (i.e., AoA) estimation in (a) and the range estimation error caused by the angle error in (b).

3.2.2 Phase-based Angle Estimation Model. The angle of arrival (AoA) refers to the direction of a tag's arrival signal with respect to an array of reader's antennas, or the direction of a reader's arrival signal with respect to an array of tags. For simplicity, we assume an antenna-array at a reader for our analysis. However, the analysis for a tag-array is similar due to the inherent symmetry in the mathematical model.

Specifically, consider a 2-element antenna array[2] as shown in Fig. 3(a). Then, the AoA θ is [1, 25]:

$$\theta = \arccos\left(\frac{\lambda\,|\phi_1 - \phi_2|}{4\pi D}\right) = f(|\phi_1 - \phi_2|), \tag{6}$$

where, ϕ_1 and ϕ_2 are phases of a tag's signal measured at two antennas, λ is the wavelength, and D ($< \lambda/4$) is the distance between two antennas. Considering a phase noise $\Delta\phi$ in the differential phase measurement $|\phi_1 - \phi_2|$, the AoA error can be expressed as follow:

$$E_\theta = |f(|\phi_1 - \phi_2|) - f(|\phi_1 - \phi_2| + \Delta\phi)|\,. \tag{7}$$

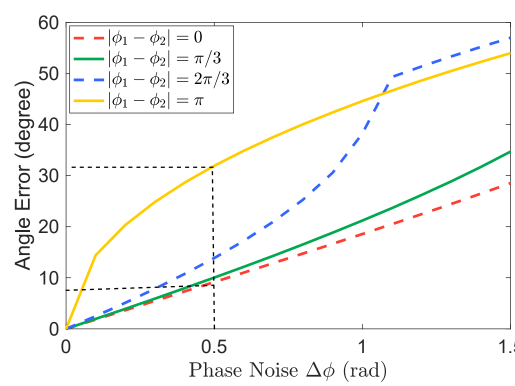

Figure 4: Impact of phase noise on the angle error.

Eqn. (7) shows that the AoA error is related to both the true phase difference $|\phi_1 - \phi_2|$ and phase noise $\Delta\phi$. Fig. 4 shows the impact of phase noise on AoA errors for different values of $|\phi_1 - \phi_2|$ and $\Delta\phi$.

[2] Note that although larger antenna arrays have better resolutions than 2-element arrays, their errors are the same for the same phase noise level.

As can be seen, even a 0.5 radians phase noise level would result in an AoA error of 9-32°. Such a large AoA error causes significant localization errors. For example, when the distance between the tag and the antenna-array is 5 m ($d = 5$), a phase noise level of 0.5 radians can result in a distance (or range) error of $\sim d \cdot E_{\theta}$= 0.8-2.8 m, as shown in Fig. 3(b).

3.3 Summary

This section demonstrates that phase/RSS noise can significantly impact the accuracy of range and angle estimations. For example, even a fairly low noise level of 0.5 radians in phase or 2 dB in RSS can result in an angle estimation error of 9-32° or a range estimation error of 1.1 m. However, many applications require highly-accurate distance and angle measurements. For example, sub-meter accuracy is required for human body localization [42] and decimeter-level accuracy is needed for baggage sorting [45] or locating a book in a stack [40]. Similarly, a few degrees of error in an angle estimation could make a robotic arm fail an assembly task [39], or result in an accident in a cargo hold due to the failure in a tilt alarm [16]. It is worth noting that some RFID systems use a fingerprint-based method (i.e., a 'training and testing' approach) instead of a phase/RSS model to estimate distance and AoA. However, this approach is also not robust, given that phase noise and RSS noise can vary as large as π radians and 10 dB due to small changes in a tag's orientation or flexing (see Section 4). Thus, test data is likely to differ significantly from training data unless the environment and tag orientation is precisely controlled.

4 HOW ROBUST ARE PHASE AND RSS?

We now present experiments that investigate the degree to which phase and RSS readings might change in realistic settings. Note that most RFID readers support multiple antennas. Thus, some existing studies use *differential* phase and *differential* RSS for AoA and distance estimations. Thus, in addition to absolute values, we also conduct experiments to test the level of variation in differential phase and RSS values between two reader antennas. We first describe our experimental test-bed and then detail the results for five different RFID tag types in seven use cases and four environments.

4.1 Test-bed Setup

Hardware: An Impinj Speedway R420 reader [19] is employed without any hardware or firmware modification. The reader operates in a frequency range of 902.75–927.25 MHz. The reader uses two directional antennas with a 9 dBi gain and 63° beam widths of elevation and azimuth [3]. The distance between the two antennas is 8 cm (< quarter-wavelength). Five types of widely used tags, as shown in Fig. 5 and Table 1, are tested.

Table 1: TAG TYPES

Type	Description
1	Avery Dennison AD-227M5 [5]
2	Avery Dennison AD-383u7 [6]
3	Alien Squiggle ALN-9740 [2]
4	SMARTRAC Frog 3D [37]
5	Avery Dennison AD-172u7 [4]

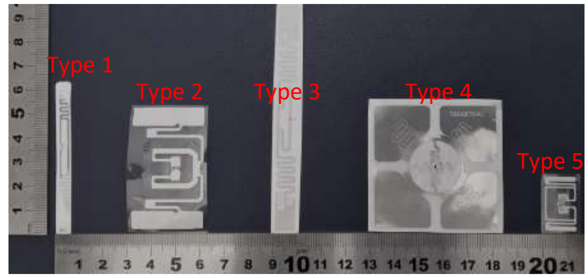

Figure 5: The five types of RFID tags used in our experiments.

Software: The software runs on a laptop and is implemented in C# and MATLAB. The laptop communicates with the RFID reader via an Ethernet cable using a low-level reader protocol [21]. Tag backscatter packets, which contain phase and RSS information, are received by two antennas at the reader and forwarded to the laptop for analysis. Note that commercial readers perform frequency hopping to comply with FCC regulations [11], which creates inconsistency between measurements. To avoid this, following best practice, we use a software filter to only collect packets from the same channel.

Table 2: DEFAULT EXPERIMENTAL SETUP

Parameter	Value
Reader transmission power	32.5 dBm
Distance between tag and reader's antenna	1.5 m
Deployment height of a reader's antenna	1.5 m
Deployment height of a tag	1.5 m
Deployment angle of a tag	90° (see Figure 7(e))
Orientation of a tag	'XY1' (see Figure 7(a))
Bending shape of a tag	Flat (see Figure 7(b))
Surface material that a tag is attached to	Wood
Experimental environment	Classroom

Deployment: We deploy one reader and one tag using the default setup values shown in Table 2.

Methodology: We evaluate the impact of different environments and setup parameters (i.e., use cases) on both the absolute phase and RSS readings (with a single antenna), and the differential phase and RSS values (with two antennas). Specifically, in an open classroom environment as shown in Fig. 6(a), we evaluate the impact of seven parameters:

(1) Orientation,
(2) Bending or flexing,
(3) Surface material that a tag is attached to,
(4) Deployment angle, i.e., where the tag is in the antenna's beam (see Figure 7(e)),
(5) Deployment height of a tag above the floor,
(6) Small movements,
(7) Distance between a tag and the reader's antenna.

For each evaluation, we change one parameter and keep the other parameters the same as the default. More than 100 phase and RSS readings are collected at each antenna and for each experiment.

To evaluate the impact of the environment, we perform experiments in four different environments: a classroom, an office area,

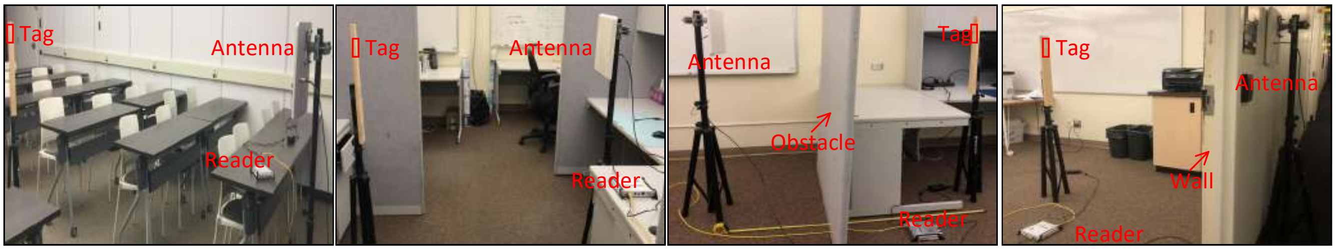

(a) Classroom scene (b) Office scene (c) NLoS scene (d) Through-wall scene

Figure 6: Four environments: (a) a classroom, (b) an office area, (c) an NLoS scenario, and (d) a through-wall scenario.

(a) (b) (c) (d) (e)

Figure 7: Deployment details for five use cases: (a) possible orientations, (b) possible bending shapes, (c) surface materials that a tag may be attached to, (d) small movements of a tag, and (e) deployment angles of a tag *w.r.t* the reader's antenna.

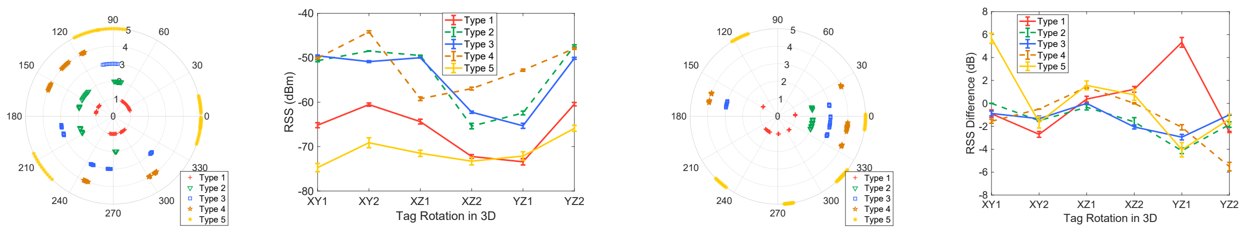

(a) Absolute phase (b) Absolute RSS (c) Differential phase (d) Differential RSS

Figure 8: Impact of tag orientations.

a non-line-of-sight (NLoS) scenario, and a through-wall scenario, as shown in Fig. 6. Finally, we repeat all the evaluations for five different tag types, as shown in Fig. 5. To aid other researchers in repeating our experiments and validating our conclusions, we have made our testing software and all the raw experimental data openly available at https://www.dropbox.com/s/z34h0lk7bc8x0p0/Raw-data-and-Software-code.zip?dl=0. We now discuss our experimental results.

4.2 Impact of Tag Orientation

In practice, RFID tags are attached to objects (such as books, baggage, etc.) that can be moved. Hence, it is essential to evaluate the impact of tag orientation on phase and RSS readings. To do so, each antenna collects the RSS and phase of a tag's backscatter signal for six different tag orientations while the other parameters are at their default values. Specifically, we consider a 3D space with three 2D planes as shown in Fig. 7(a), where the 'XY plane' is facing the reader's antenna. For each 2D plane, we deploy one of five different tag types along two different axes (such as XY1 and XY2) and then collect phase and RSS readings.

Fig. 8 shows the results of this evaluation.[3] It is evident that changes in a tag's orientation can cause significant changes in absolute and differential values of both RSS and phase. For example, for a Type 1 tag, absolute and differential phase readings can vary by as much as π radians; the absolute RSS changes as much as 10 dB, and the differential RSS changes from -3 dB to 6 dB with a gap of 9 dB. As discussed in Section 3.2, a phase or RSS noise level (i.e., variation) larger than 0.5 radians or 2 dB would result in large angle or range estimation errors. Thus, this experiment implies that RFID-based systems (such as localization and tracking systems) using Type 1 tags would not meet the desired level of accuracy even when the tag's location is fixed, if there can be changes in the tag orientation. Therefore, relying on phase and RSS alone may not sufficient to estimate the location of a tag. To solve this problem, one could design an orientation-aware RFID system that

[3] In Figures 8(b) and 8(d), lines connecting data points have been added for visual clarity.

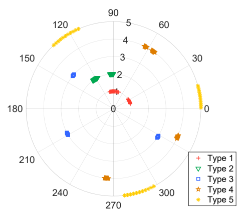

(a) Absolute phase

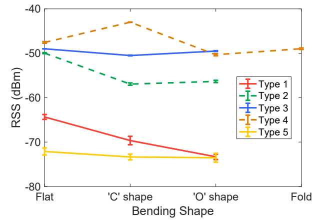

(b) Absolute RSS

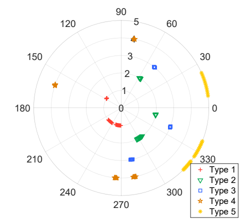

(c) Differential phase

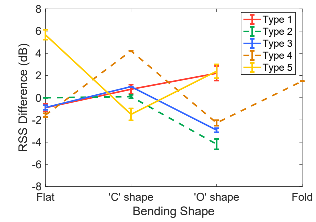

(d) Differential RSS

Figure 9: Impact of a tag's bending. Note that tags of Type 1, 2, 3 and 5 are not readable when they are folded.

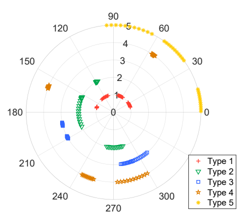

(a) Absolute phase

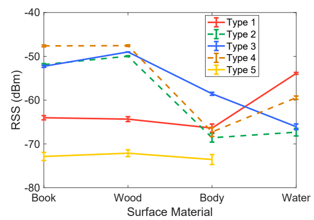

(b) Absolute RSS

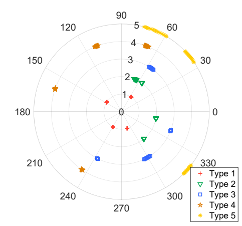

(c) Differential phase

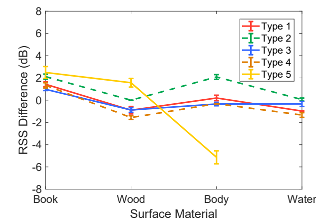

(d) Differential RSS

Figure 10: Impact of surface materials.

takes changes in the tag orientation into account when trying to localize it [22]. Note also that the variation in differential phase and RSS values is generally lower than the variation in absolute values. This suggests differential measurements are generally superior to absolute measurements. Finally, note that some tags, such as Type 2 tags, have much lower differential phase errors than Type 1 tags. Thus, careful tag selections can mitigate the impact of tag orientations.

4.3 Impact of Tag Bending Shape

Objects in the real world vary in their surface geometry. For example, the surface of a book is flat whereas the surface of a cup or bottle is highly curved. Thus, flexible RFID tags placed on the surface of an object could bend or flex. In this set of experiments, we test the impact of a tag's bending shape on its absolute and differential phase and RSS readings. Specifically, we evaluate four bending shapes shown in Fig. 7(b): 'Flat' and 'C-shape' represent typical bending shapes, whereas 'O-shape' and 'Fold' are more extreme levels of flexion.

Fig. 9 shows the impact of tag bending shapes. It is clear that the tag flexion or bending can significantly impact its phase and RSS measurements, depending on tag types. For example, the absolute and differential phase values of a Type 3 tag change by more than $\pi/2$ radians with different bending shapes. In addition, the absolute and differential RSS values of a Type 1 tag can vary by as much as 6 dB. We also find that the tags of Type 1, Type 2, Type 3 and Type 5 are not readable when they are folded (as they might be, for example, inside a book).

These results demonstrate that tag shape could have a significant impact on phase and RSS readings. As a result, the accuracy of RFID-based systems might degrade when tag shape changes. Therefore, existing RFID based systems require the user to avoid changing the shape of a tag. Moreover, careful choice of tag types and signal features can mitigate the impact of bending: for example, the tag Type 3 shows little variation in absolute or differential RSS values for common levels of bending.

4.4 Impact of Surface Material

Different objects are made from different materials. Thus, it is inevitable that RFID tags will be attached to different surface materials in real-world deployments. To evaluate the impact of surface materials on a tag placed on them, we attach RFID tags to four kinds of surfaces[4]: a book, a piece of wood, a human subject, and a bottle of water, as shown in Fig. 7(c).

The results in Fig. 10 demonstrate that, when the surface material changes, the absolute and differential phase values of all tags vary by as large as $\pi/2$ radians. Moreover, both the absolute and differential RSS values can vary by more than 5 dB when the surface material changes from an insulator (e.g., wood) to a conductor (e.g., water), depending on tag types. Again, differential RSS values exhibit far lower levels of variations than absolute values.

We make two observations based on the results. First, RSS-based RFID applications will work well only when the tag is attached to an insulator. Second, phase-based applications may not meet required accuracy goals if the tags used in the application are attached to

[4]We also tested the surfaces of a smart-phone and a metal plate. However, most tags are not readable when they are attached to metal surfaces.

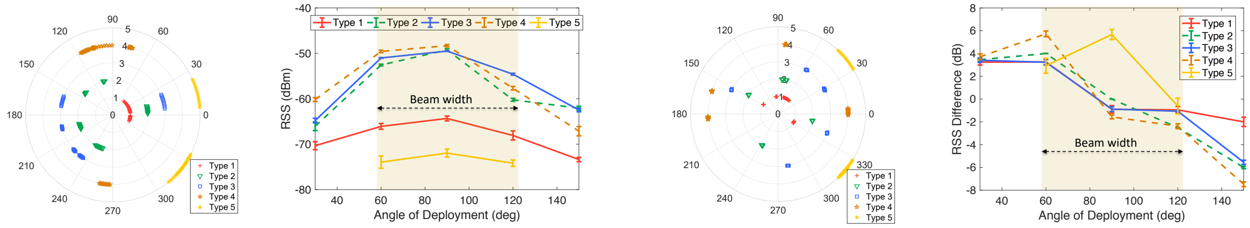

(a) Absolute phase (b) Absolute RSS (c) Differential phase (d) Differential RSS

Figure 11: Impact of deployment angle. Tags of Type 5 are not readable when the deployment angle is 30° or 150°.

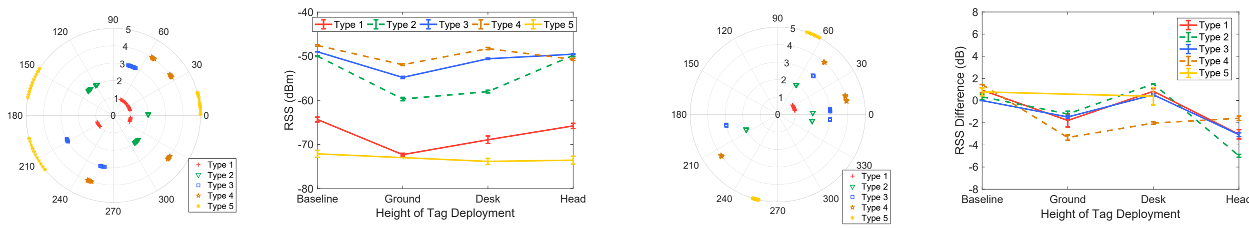

(a) Absolute phase (b) Absolute RSS (c) Differential phase (d) Differential RSS

Figure 12: Impact of deployment heights.

different surfaces, such as a book or a glass of water, even if they are co-located.

4.5 Impact of Deployment Angle

In most RFID applications, readers are fixed while tags are mobile. Thus, the location of a tag in the reader's receiving beam, which we call the 'deployment angle' (see Figure 7(e)) is likely to change. In this experiment, we evaluate the impact of deployment angles on a tag's phase and RSS readings. Specifically, we test five different deployment angles: 30°, 60°, 90°, 120° and 150°, as shown in Fig. 7(e), while keeping the distance between the tag and the reader antenna the same (i.e., 1.5 m). The tag faces the reader's antenna when the deployment angle is 90°.

Fig. 11(a)–(b) show that absolute phase and RSS values can vary by as much as π radians and 15 dB (for a Type 3 tag) when the deployment angle changes. In theory, the absolute phase values should not change because the distance between the tag and the reader is constant. The observed RSS changes are due to the directional property of the reader's antenna. Specifically, the antenna has a beam width of 63°. Therefore, when a tag is located outside of the antenna's beam, the gain of the antenna decreases significantly, resulting in change in RSS. Moreover, since we gather measurements for only five different deployment angles, we should observe five symmetric clusters in the differential phase measurements. However, the results in Fig. 11(c) are not consistent with this. For example, for Type 1, Type 2 and Type 4 tags, the number of clusters is less than five and they are not symmetric.

Overall, the results imply that changes in the deployment angle of a tag can result in very noisy phase and RSS readings. Unfortunately, these changes in the deployment angle are unavoidable in practical situations. As a result, some applications, such as localization and tracking, are bound to suffer large errors when a tag moves across the boundary of an antenna's beam.[5] One should select an appropriate antenna beam width based on the application's required coverage area.

4.6 Impact of Deployment Height

In most RFID applications, tags will be deployed at different heights. For example, in a library, RFID tags are attached to books placed in different shelves. To evaluate the impact of a tag's height on phase and RSS readings, we keep the tag's location in 2D space (i.e., the tag's location is unchanged if we project the location of the tag to the ground), and only change its deployment height with four values: 'Ground' (0 m), 'Desk' (1.2 m), 'Baseline' (1.5 m) and 'Overhead' (2 m).

Fig. 12 shows that the absolute and differential values of both RSS and phase can change significantly with different tag heights. For example, the differential phase and absolute RSS variations of the Type 2 tag can be as much as $\pi/2$ radians and 8 dB, respectively. These phase and RSS variations are not surprising, since the tag-to-reader distance changes when changing the deployment height of a tag.

Since even a small change in the height of a tag can significantly impact an RFID system's range and AoA estimates, most existing RFID-based localization and tracking systems require tags and reader antennas to be deployed in the same 2D plane. However, to make these systems practical, one should analyze RFID signal features in *3D* space, where a tag's deployment height can indeed

[5]Note, it is impossible to differentiate whether an RFID tag is inside or outside of the antenna's beam based on the RSS measurement.

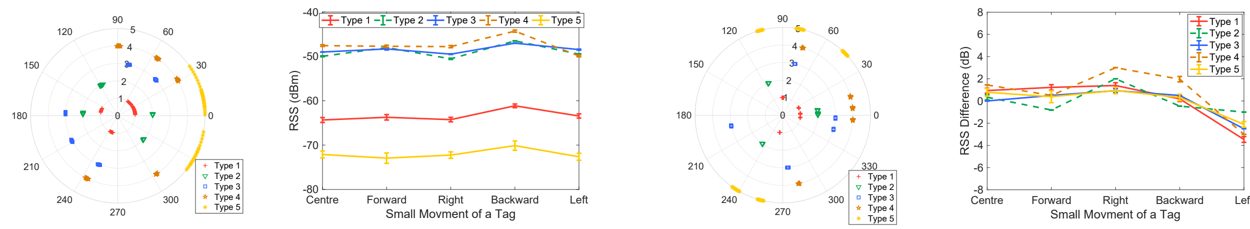

(a) Absolute phase (b) Absolute RSS (c) Differential phase (d) Differential RSS

Figure 13: Impact of small movements

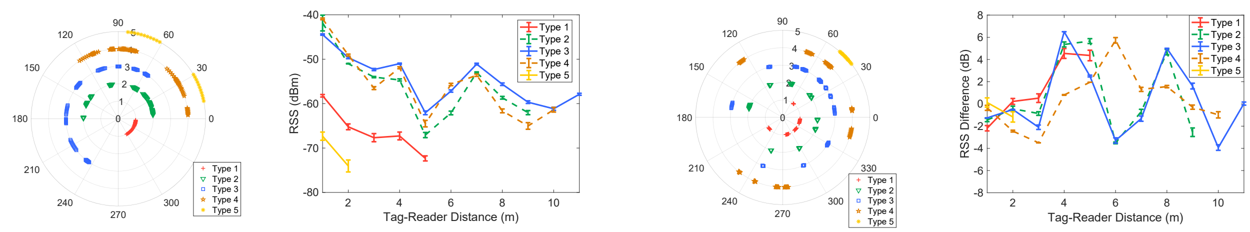

(a) Absolute phase (b) Absolute RSS (c) Differential phase (d) Differential RSS

Figure 14: Impact of tag-reader distances.

change. Moreover, some tag types and signal features are less sensitive to changes in the deployment height than others. For example, the absolute RSS values of Type 3 tags does not vary much with changes in the deployment height.

4.7 Impact of Small Movements

In many scenarios, locations of objects change slightly during usage. Thus, we evaluate the impact of small movements on the phase and RSS readings of a tag. To do so, each reader antenna measures RSS and phase while we move a tag ~10 cm away from its default location, as shown in Fig. 7(d).

Fig. 13 shows that small movements do not significantly affect a tag's absolute and differential RSS readings because RSS is a coarse-grained feature. However, the phase is sensitive to changes in a tag's location. For example, a 16 cm displacement can result in up to 2π radians of phase changes. Moreover, both absolute and differential phase readings of all tag types can change by as much as π radians.

These results imply that RSS-based RFID application systems are robust to small tag movements, while phase-based RFID application systems are likely to encounter significant errors when tag location changes even slightly. For example, in an RFID-based touch sensing application, when one moves the tag slightly, touch detection would continue to be robust if RSS is used for detection. However, phase-based touch detection will suffer errors since it requires the locations of tags to be fixed [26].

4.8 Impact of Tag-Reader Distance

In many RFID applications, such as localization, tracking and activity recognition, distances between tags and the reader may change. Thus, we evaluate the impact of tag-to-reader distance on RSS and phase by varying the distance between a reader and a tag from 1 m to 11 m, while other parameters are kept at their default values.

Fig. 14 shows that absolute and differential values of both phase and RSS readings vary when the distance between a tag and a reader changes. This observation is consistent with theoretical phase/RSS models. Our results also show that different tags have different reading ranges. For example, the range of a Type 5 tag is limited to 2 m, while Type 3 and Type 4 tags are readable even at a distance of 10 m. The results motivate us to select different tag types based on the reading range requirement of different applications.

4.9 Impact of the Environment

Due to the diversity of their applications, RFID tags could be deployed in different environments. We evaluate the impact of four typical environments (see Fig. 6) on the phase and RSS readings of a tag. For tractability, we only study changes in a tag's orientation in differing environments, but expect to see similar observations for other cases as well.

Fig. 15–Fig. 19 show absolute and differential values for both phase and RSS readings for five type tags in four different environments. As can be seen, these values changes by as much as π radians and 10 dB, respectively, for different tag orientations in all four environments.

Overall, these results imply that existing RFID-based application systems may not be able to guarantee accuracy even for the same tag orientation as the deployment environment changes, due to the large changes in both the absolute and differential phase and RSS readings. For example, an RFID-based localization system that works well in an open classroom, may have large errors in a library

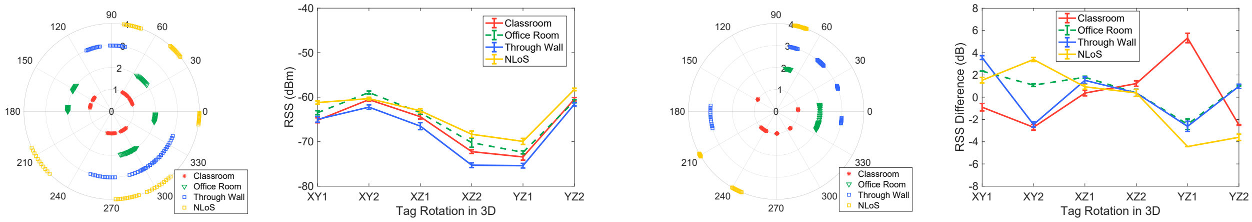

(a) Absolute phase (b) Absolute RSS (c) Differential phase (d) Differential RSS

Figure 15: Impact of different environments on the phase and RSS readings of a Type 1 tag, when the tag has different orientations.

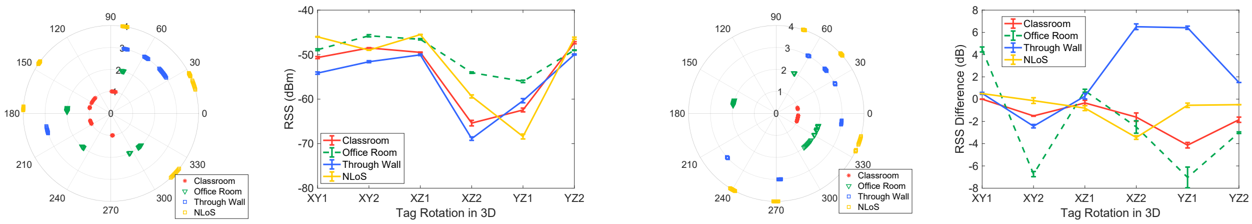

(a) Absolute phase (b) Absolute RSS (c) Differential phase (d) Differential RSS

Figure 16: Impact of different environments on the phase and RSS readings of a Type 2 tag, when the tag has different orientations.

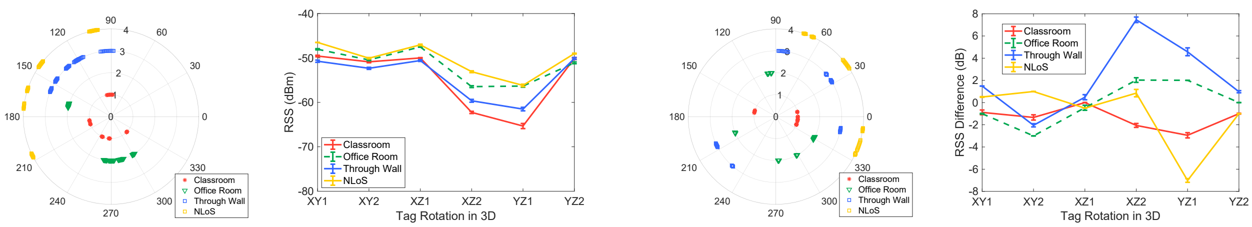

(a) Absolute phase (b) Absolute RSS (c) Differential phase (d) Differential RSS

Figure 17: Impact of different environments on the phase and RSS readings of a Type 3 tag, when the tag has different orientations.

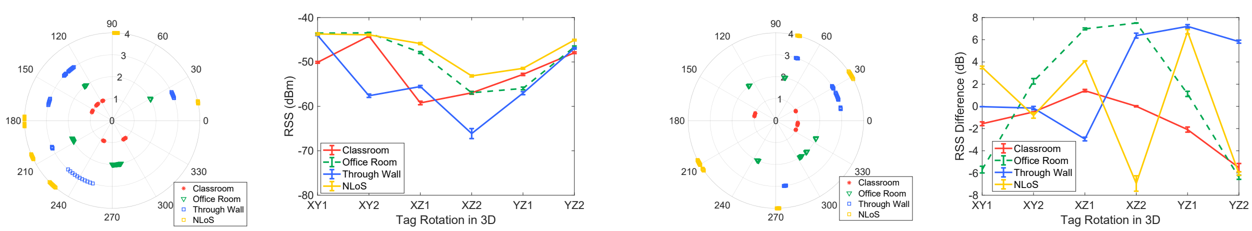

(a) Absolute phase (b) Absolute RSS (c) Differential phase (d) Differential RSS

Figure 18: Impact of different environments on the phase and RSS readings of a Type 4 tag, when the tag has different orientations.

environment due to large phase and RSS variations caused by the rich multipath effect.

4.10 Observations

Our experiments conclusively demonstrate that, depending on the type of tag, even small changes in the environment and system setup can significantly impact absolute and differential values of

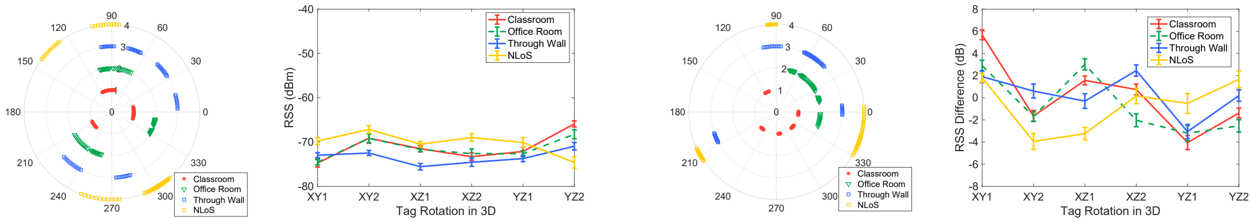

(a) Absolute phase (b) Absolute RSS (c) Differential phase (d) Differential RSS

Figure 19: Impact of different environments on the phase and RSS readings of a Type 5 tag, when the tag has different orientations.

both phase and RSS readings of RFID tags, resulting in significant errors in the accuracy of resultant RFID systems. Based on these results, we make the following two observations:

Observation 1: Variations in absolute and differential values of both phase and RSS readings for a *fixed* setup and environment are relatively small: i.e., error bars are quite small in most cases. This confirms the high accuracy reported by developers of past RFID-based applications but *only* when tag geometry and the RF environment is tightly controlled. Our results imply that this repeatability does *not* imply robustness of these applications in practice.

Observation 2: The absolute and differential values of both phase and RSS readings of RFID tags can vary significantly when tag geometry and environmental conditions change. In most cases, variations in absolute and differential values of both phase and RSS readings are much larger than the noise level of 0.5 radians and 2 dB discussed in Section 3.2. This implies that when the RF environment and parameters such as tag orientation, tag-reader angle, or exact deployment height change, most existing RFID-based systems will be unable to meet application requirements. *This validates our research hypothesis.*

5 DISCUSSION

Despite our negative results, we believe that there is still hope for designing robust RFID systems that can meet application requirements. In this section, we discuss how to improve the robustness of RFID systems by choosing the right signal features and tag types.

5.1 Choosing Appropriate Signal Parameters

As discussed in Section 4, even when the distance between a tag and a reader is fixed, the absolute and differential values of both phase and RSS readings of a tag vary depending on the environment, tag's orientation, etc. Therefore, to use phase and RSS measurements for localization and sensing applications, current systems need frequent re-calibration, which is impractical. However, depending on the application, one might find other signal features, which are more robust than absolute and differential measurements of RSS and phase. For example, Wang *et al.* [38] presented a new signal feature, the Differential Minimum Response Threshold (DMRT),[6] which is much more robust than both absolute and differential RSS measurements. Similarly, Xiao *et al.* [44] achieved fine-grained RFID localization in complex environments by attaching two RFID tags to one object. By using two tags, they both calibrate and compensate for the impact of a tag's orientation on its phase and RSS measurements. Thus, with their approach, high localization accuracy is feasible. We believe that for other applications, such as gesture sensing and device-free sensing, it might be similarly possible to find and design new signal features that are much more robust than RSS and phase parameters.

5.2 Choosing Appropriate Tag Types

Our experimental results (presented in Section 4) show that the robustness of RSS and phase measurements significantly depends on tag types. Therefore, it is important to choose the right type of tags for the targeted application. For example, Fig. 14(b) shows that Type 3 and Type 4 tags provide a much longer working range than the other three types of tags. Therefore, if an application requires a long working range, one should select these tags. On the other hand, although Type 5 tag has a very short range, our results in Fig. 19(b) show that this tag has more robust RSS measurements in different scenarios compared to the other tags. Therefore, one should choose Type 5 tags if the application requires a short range but robust RSS measurements. In a word, to choose the right tag type, both the application requirements and the signal features used in the application must be taken into account.

6 CONCLUSION

This paper attempts to answer the question of why novel RFID-based application systems remain research prototypes and have not been widely deployed in practice. We find that existing RFID systems primarily rely on phase and RSS measurements of RFID backscatter signals to enable applications such as localization and sensing. However, even a minor change in the environment or a tag's geometry (such as rotating or bending the tag) can cause large variations in both the absolute and differential values of phase and RSS readings, which can result in significant range and angle estimation errors. Therefore, the accuracy of existing systems may not meet application requirements in practice. In addition to this strong negative result, we have also presented some insights into designing robust RFID systems based on a proper selection of tag type and signal feature. We believe that our results and insights will help the research community in designing robust and practical RFID systems which can meet application requirements in real deployments.

[6]DMRT is the difference between the minimum transmission power levels of a reader to activate two co-located RFID tags.

ACKNOWLEDGMENT

We would like to thank the shepherd Jeremy Gummeson and the anonymous reviewers for their valuable feedback on this paper. We also thank Costin Ograda-Bratu for his help with experiments.

REFERENCES

[1] Omid Abari, Deepak Vasisht, Dina Katabi, and Anantha Chandrakasan. 2015. Caraoke: An e-toll transponder network for smart cities. In *ACM SIGCOMM Computer Communication Review*, Vol. 45. 297–310.
[2] Alien Technology Corp. 2017. UHF ALN-9740 tag. https://www.atlasrfidstore.com/alien-squiggle-rfid-white-wet-inlay-aln-9740-higgs-4/. (2017). Last accessed: July 17, 2018.
[3] Atlasrfidstore. 2018. RFMAX RFID Race Timing Antenna. https://www.atlasrfidstore.com/rfmax-rfid-race-timing-antenna-kit-15-ft-cable/. (2018). Last accessed: July 27, 2018.
[4] Avery Dennison Corp. 2017. UHF AD-172u7 tag. http://rfid.averydennison.com/content/dam/averydennison/rfid/Global/Documents/datasheets/AD-172u7-datasheet-v1.pdf. (2017). Last accessed: July 17, 2018.
[5] Avery Dennison Corp. 2017. UHF AD-227m5 tag. http://rfid.averydennison.com/content/dam/averydennison/rfid/Global/Documents/datasheets/AD-227m5-Datasheet-v1.pdf. (2017). Last accessed: July 17, 2018.
[6] Avery Dennison Corp. 2017. UHF AD-383u7 tag. http://rfid.averydennison.com/content/dam/averydennison/rfid/Global/Documents/datasheets/AD-383u7-Datasheet-v1.pdf. (2017). Last accessed: July 17, 2018.
[7] Rahul Bhattacharyya, Christian Floerkemeier, and Sanjay Sarma. 2010. Low-cost, ubiquitous RFID-tag-antenna-based sensing. *Proc. IEEE* 98, 9 (2010), 1593–1600.
[8] Rahul Bhattacharyya, Christian Floerkemeier, and Sanjay Sarma. 2010. RFID tag antenna based sensing: Does your beverage glass need a refill?. In *Proc. IEEE International Conference on RFID*. 126–133.
[9] Kevin Bouchard, Abdenour Bouzouane, and Bruno Bouchard. 2014. Gesture recognition in smart home using passive RFID technology. In *Proc. ACM International Conference on Pervasive Technologies Related to Assistive Environments*. 12–19.
[10] Michael Buettner, Richa Prasad, Matthai Philipose, and David Wetherall. 2009. Recognizing daily activities with RFID-based sensors. In *Proc. ACM International Conference on Ubiquitous Computing*. 51–60.
[11] Michael Buettner and David Wetherall. 2010. A Gen 2 RFID monitor based on the USRP. *ACM SIGCOMM Computer Communication Review* 40, 3 (2010), 41–47.
[12] Han Ding, Jinsong Han, Alex X Liu, Jizhong Zhao, Panlong Yang, Wei Xi, and Zhiping Jiang. 2015. Human object estimation via backscattered radio frequency signal. In *Proc. IEEE INFOCOM*. 1652–1660.
[13] Han Ding, Longfei Shangguan, Zheng Yang, Jinsong Han, Zimu Zhou, Panlong Yang, Wei Xi, and Jizhong Zhao. 2015. Femo: A platform for free-weight exercise monitoring with RFIDs. In *Proc. ACM Conference on Embedded Networked Sensor Systems*. 141–154.
[14] Joshua D Griffin and Gregory D Durgin. 2009. Complete link budgets for backscatter-radio and RFID systems. *IEEE Antennas and Propagation Magazine* 51, 2 (2009).
[15] Gaurangi Gupta, Bhanu Pratap Singh, Amrita Bal, Deepam Kedia, and AR Harish. 2014. Orientation detection using passive UHF RFID technology. *IEEE Antennas and Propagation Magazine* 56, 6 (2014), 221–237.
[16] Larry L Hall and Duane S Schmoker. 2006. Cargo lock and monitoring apparatus and process. (May 2 2006). US Patent 7,038,585.
[17] Cory Hekimian-Williams, Brandon Grant, Xiuwen Liu, Zhenghao Zhang, and Piyush Kumar. 2010. Accurate localization of RFID tags using phase difference. In *Proc. IEEE International Conference on RFID*. 89–96.
[18] Elisabeth Ilie-Zudor, Zsolt Kemény, Fred Van Blommestein, László Monostori, and André Van Der Meulen. 2011. A survey of applications and requirements of unique identification systems and RFID techniques. *Elsevier Computers in Industry* 62, 3 (2011), 227–252.
[19] Impinj. 2010. Impinj R420 Readers. http://www.Impinj.com/products/readers/. (2010). Last accessed: June 27, 2018.
[20] Impinj. 2013. Impinj RFID Reader Low Level Data Support. https://support.impinj.com/hc/en-us/articles/202755318-Application-Note-Low-Level-User-Data-Support. (2013). Last accessed: July 17, 2018.
[21] EPCglobal Inc. 2007. Low Level Reader Protocol, Version 1.0. 1. (2007).
[22] Chengkun Jiang, Yuan He, Xiaolong Zheng, and Yunhao Liu. 2018. Orientation-aware RFID tracking with centimeter-level accuracy. In *Proc. ACM/IEEE IPSN*. 290–301.
[23] Hanchuan Li, Eric Brockmeyer, Elizabeth J Carter, Josh Fromm, Scott E Hudson, Shwetak N Patel, and Alanson Sample. 2016. PaperID: A technique for drawing functional battery-free wireless interfaces on paper. In *Proc. ACM Conference on Human Factors in Computing Systems (CHI)*. 5885–5896.
[24] Hanchuan Li, Can Ye, and Alanson P Sample. 2015. IDSense: A human object interaction detection system based on passive UHF RFID. In *Proc. ACM Conference on Human Factors in Computing Systems*. 2555–2564.
[25] Sophocles J Orfanidis. 2002. Electromagnetic waves and antennas. (2002).
[26] Swadhin Pradhan, Eugene Chai, Karthikeyan Sundaresan, Lili Qiu, Mohammad A Khojastepour, and Sampath Rangarajan. 2017. RIO: A Pervasive RFID-based Touch Gesture Interface. In *Proc. ACM MobiCom*. 261–274.
[27] Das Raghu. 2017. RFID Forecasts, Players and Opportunities 2017-2027. https://www.idtechex.com/research/reports/rfid-forecasts-players-and-opportunities-2017-2027-000546.asp. (2017). Last accessed: July 27, 2018.
[28] Alanson P Sample, Daniel J Yeager, and Joshua R Smith. 2009. A capacitive touch interface for passive RFID tags. In *Proc. IEEE International Conference on RFID*. 103–109.
[29] T Sanpechuda and L Kovavisaruch. 2008. A review of RFID localization: Applications and techniques. In *Proc. IEEE International Conference on Electrical Engineering/Electronics, Computer, Telecommunications and Information Technology*. 769–772.
[30] Longfei Shangguan and Kyle Jamieson. 2016. The design and implementation of a mobile RFID tag sorting robot. In *Proc. ACM MobiSys*. 31–42.
[31] Longfei Shangguan and Kyle Jamieson. 2016. Leveraging electromagnetic polarization in a two-antenna whiteboard in the air. In *Proc. ACM CoNEXT*. 443–456.
[32] Longfei Shangguan, Zhenjiang Li, Zheng Yang, Mo Li, and Yunhao Liu. 2013. Otrack: Order tracking for luggage in mobile RFID systems. In *Proc. IEEE INFOCOM*. 3066–3074.
[33] Longfei Shangguan, Zheng Yang, Alex X Liu, Zimu Zhou, and Yunhao Liu. 2015. Relative Localization of RFID Tags using Spatial-Temporal Phase Profiling.. In *Proc. USENIX NSDI*. 251–263.
[34] Longfei Shangguan, Zimu Zhou, and Kyle Jamieson. 2017. Enabling gesture-based interactions with objects. In *Proc. ACM MobiSys*. 239–251.
[35] Longfei Shangguan, Zimu Zhou, Xiaolong Zheng, Lei Yang, Yunhao Liu, and Jinsong Han. 2015. ShopMiner: Mining customer shopping behavior in physical clothing stores with COTS RFID devices. In *Proc. ACM Conference on Embedded Networked Sensor Systems*. 113–125.
[36] Ali Asghar Nazari Shirehjini, Abdulsalam Yassine, and Shervin Shirmohammadi. 2012. An RFID-based position and orientation measurement system for mobile objects in intelligent environments. *IEEE Transactions on Instrumentation and Measurement* 61, 6 (2012), 1664–1675.
[37] Smartrac Corp. 2013. UHF SMARTRAC Frog 3D tag. https://www.atlasrfidstore.com/smartrac-frog-rfid-wet-inlay-monza-4d/. (2013). Last accessed: July 17, 2018.
[38] Ju Wang, Omid Abari, and Srinivasan Keshav. 2018. Challenge: RFID Hacking for Fun and Profit. In *Proc. ACM MobiCom*. 1–10.
[39] Jue Wang, Fadel Adib, Ross Knepper, Dina Katabi, and Daniela Rus. 2013. RF-compass: Robot object manipulation using RFIDs. In *Proc. ACM MobiCom*. 3–14.
[40] Jue Wang and Dina Katabi. 2013. Dude, where's my card?: RFID positioning that works with multipath and non-line of sight. 43, 4 (2013), 51–62.
[41] Ju Wang, Jie Xiong, Xiaojiang Chen, Hongbo Jiang, Rajesh Krishna Balan, and Dingyi Fang. 2017. TagScan: Simultaneous target imaging and material identification with commodity RFID devices. In *Proc. ACM MobiCom*. 288–300.
[42] Ju Wang, Jie Xiong, Hongbo Jiang, Xiaojiang Chen, and Dingyi Fang. 2017. D-Watch: Embracing "Bad" multipaths for device-free localization with COTS RFID devices. *IEEE/ACM Transactions on Networking (TON)* 25, 6 (2017), 3559–3572.
[43] Teng Wei and Xinyu Zhang. 2016. Gyro in the air: tracking 3D orientation of batteryless internet-of-things. In *Proc. ACM MobiCom*. 55–68.
[44] Fu Xiao, Zhongqin Wang, Ning Ye, Ruchuan Wang, and Xiang-Yang Li. 2018. One more tag enables fine-grained RFID localization and tracking. *IEEE/ACM Transactions on Networking (TON)* 26, 1 (2018), 161–174.
[45] Lei Yang, Yekui Chen, Xiang-Yang Li, Chaowei Xiao, Mo Li, and Yunhao Liu. 2014. Tagoram: Real-time tracking of mobile RFID tags to high precision using COTS devices. In *Proc. ACM MobiCom*. 237–248.
[46] Lei Yang, Yao Li, Qiongzheng Lin, Huanyu Jia, Xiang-Yang Li, and Yunhao Liu. 2017. Tagbeat: Sensing Mechanical Vibration Period With COTS RFID Systems. *IEEE/ACM Transactions on Networking (TON)* 25, 6 (2017), 3823–3835.
[47] Lei Yang, Qiongzheng Lin, Xiangyang Li, Tianci Liu, and Yunhao Liu. 2015. See through walls with cots RFID system. In *Proc. ACM MobiCom*. 487–499.
[48] Junyi Zhou and Jing Shi. 2009. RFID localization algorithms and applications–a review. *Springer Journal of intelligent manufacturing* 20, 6 (2009), 695.
[49] Yongpan Zou, Jiang Xiao, Jinsong Han, Kaishun Wu, Yun Li, and Lionel M Ni. 2017. Grfid: A device-free RFID-based gesture recognition system. *IEEE Transactions on Mobile Computing* 16, 2 (2017), 381–393.